Study of the Thermal Behavior of the Complexation between Norfloxacin Drug with ZrO^{2+} and UO$_2$$^{2+}$ Ions: TGA and DTG Investigations

El-Megharbel S. M. [1*], Abdel Majid A. Adam[2], Moamen S. Refat [2,3]

[1]Department of Chemistry, Faculty of Science, Zagazig University, Zagazig, Egypt
[2]Department of Chemistry, Faculty of Science, Taif University, 888 Taif, Saudi Arabia
[3]Department Chemistry, Faculty of Science, Port Said University, Port Said, Egypt
samyelmegharbel@yahoo.com

Abstract: The interactions of ZrO^{2+} and UO$_2$$^{2+}$ ions with the second-generation fluoroquinolone, norfloxacin (NFX) were studied. The obtained complexes were characterized by elemental analysis, electrical conductivity and infrared spectra. The IR spectra of the isolated solid complexes indicated that NFX act as deprotonated bidentate ligand bound to the metal through one of the oxygen atom of the carboxylic group and the ring carbonyl oxygen atom, forming five and six atoms ring with ZrO^{2+} and UO$_2$$^{2+}$ ions, respectively. The thermal behavior of these two complexes were investigated on the basis of thermogravimetric (TGA) and differential thermogravimetric (DTG) analyses, as well as kinetic thermodynamic parameters estimated from Coats-Redfern and Horowitz-Metzger integral methods. Infrared and thermogravimetric studies reveal the presence of coordinated water molecules. Based on the reported data, the proposed structure of the obtained complexes are [ZrO(NFX)$_2$]·4H$_2$O and [UO$_2$(NFX)$_2$]·9H$_2$O.

1. Introduction

Norfloxacin (NFX) is a second-generation fluoroquinolone, chemically named as 1-ethyl-6-fluoro-1,4-dihydro-4-oxo-7-(piperazin-1-yl)quinoline-3-carboxylic acid (Formula I) [1]. In recent years, NFX has been ranked as the second most prescribed fluoroquinolone antibacterial just next to levofloxacin in China. It is the first fluoroquinolone, which was synthesized by converting nalidixic acid into a quinolone structure, adding a fluorine atom and piperazine ring [2]. NFX is the first choice drug for the treatment of diseases caused by *Campylobacter*, *E. coli*, *Salmonella*, *Shigella*, and *V. colera*. It is used for the therapy of gonorrhea as well as eye and urinary tract infections [3-5]. NFX has a broad spectrum with antibacterial activity against both Gram-positive and Gram-negative through inhabitation of DNA gyrase [6,7], thus it extensively used in both human and veterinary medicine. NFX is active *in vitro* against many Gram-positive and Gram-negative bacteria because it urine concentration is 100-300 times higher than that in serum which largely exceeds its minimal inhibitory concentration (MIC) and minimal bactericidal concentration (MBC). It was discovered that the fluorine atom at the 6th position provides increased potency against Gram-negative organisms and the piperazine moiety at the 7th position is responsible for the antpseudomonal activity of NFX [8].

Recently, many studies and research were conducted on NFX drug such as, determination of NFX in biological samples and medicine [9-12], synthesis and structure of NFX metal complexes [13-20], the antimicrobial evaluation of NFX and its derivatives [21-24], sorption behavior [25], and photodegradation of NFX [26]. The aim of this work is to synthesize and investigate systematically the thermal behavior of norfloxacin complexes with ZrO^{2+} and UO$_2$$^{2+}$ ions. The interpretation of the thermo-kinetic behavior of these complexes were carried out through the mathematical analysis and evaluation of kinetic parameters of thermogravimetric (TGA) and its differential (DTG), such as entropy of activation, pre-exponential factors, activation energy evaluated by using Coats-Redfern and Horowitz-Metzger equations. The elemental analysis and infrared spectra were used to elucidate the mode of coordination properties of NFX with these two ions.

2. Materials and Methods

2.1 Materials

All chemicals used were of analytical reagent grade, commercially available, and were used without further purification. Norfloxacin used in this work was supplied from Egyptian International Pharmaceutical Industrial Company

(EIPICO). ZrOCl$_2$·6H$_2$O and UO$_2$(NO$_3$)$_2$·2H$_2$O were purchased from Aldrich Chemical Company.
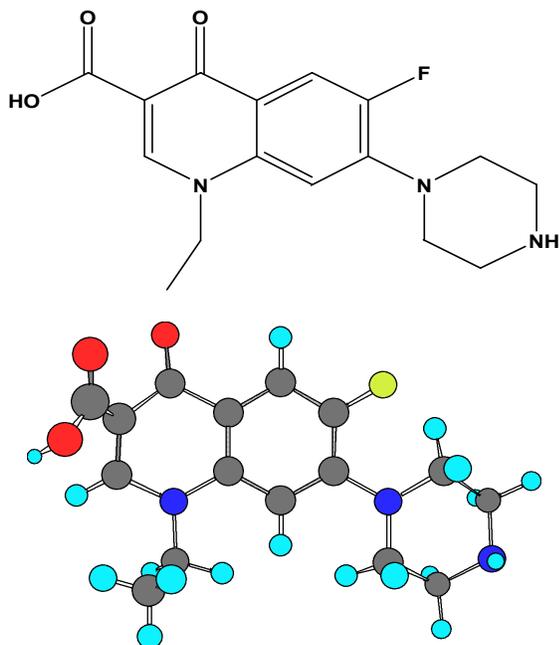
Formula I. Structure of Norfloxacin (NFX) drug.

2.2 Synthesis of NFX metal complexes

Norfloxacin (2 mmol) in mixed solvent (50/50 %) of methanol/acetone was stirred at room temperature for 20 min. A solution of 1.0 mmol of ZrOCl$_2$·6H$_2$O and UO$_2$(NO$_3$)$_2$·2H$_2$O in 5 ml of methanol was added to the NFX solution with constant stirring. The pH was adjustment at 7~8, then the resulting mixture was heated ~50 °C under reflux on a water bath for about 12 h and then cooled. The resulted solid complexes were separated from the reaction mixture by filtration, washed with methanol and dried under vacuum to a constant weight. The yields were found around 75% based on the metals salts. The compounds resulted have low solubility in water and in common organic solvents. The obtained two complexes were characterized by their elemental analysis, electrical conductivity, infrared spectra, as well as thermal analysis.

2.3 Instrumentation

The elemental analyses of carbon, hydrogen and nitrogen contents were performed by the micro analytical unit at Cairo University, Egypt, using a Perkin-Elmer CHN 2400 (USA), and the metal contents were found gravimetrically by ignition-weighted samples in atmospheric air to constant weight and definite structure. Decomposition of complexes was performed in concentrated HNO$_3$. After decomposition, the

sample was diluted with water to 100 ml, and qualitative presence of Cl$^-$ ions (in ZrO^{2+} complex) was determined by means of AgNO$_3$. Molar conductivities of freshly prepared 10^{-3} mol dm^{-3} DMSO solutions were measured on a Jenway 4010 conductivity meter. Infrared (IR) spectra (KBr discs) within the range of 4000-400 cm^{-1} for the resulted CT-complexes were carried out on a Genesis II FT-IR spectrophotometer with 30 scans and 2 cm^{-1} resolution. Thermogravimetric measurements (TG and DTG) were carried out in dynamic nitrogen atmosphere (30 ml/min.) between room temperature and 900 °C with a heating rate of 10 °C/min. using a Shimadzu TGA –50H thermal analyzers.

3. Results and discussion

3.1 Elemental analysis

The results of the elemental analysis and some physical characteristics of NFX ligand and the obtained complexes are given in Table 1. The complexes were synthesized using 1:2 (metal: ligand) mole ratio of all reactants. The elemental analysis of the complexes indicates a 1:2 metal to ligand stoichiometry, too. The analytical data indicate that the two prepared complexes contain water molecules, and the number of bound water molecules in these compounds begin different. The IR spectroscopic and thermogravimetric data also confirm water in the composition of the complexes. All of the resulted complexes are stable in air, hygroscopic, with high melting points. Investigation of the solubility of these complexes showed that they were insoluble in water, methanol, ethanol, diethylether, benzene, chloroform and carbon tetrachloride, but soluble in dimethylformamide (DMF) and dimethylsulfoxide (DMSO) with gently heating. All complexes have been prepared at high yield (76-77%), and melting points of the complexes (>300 °C) are higher than that of the ligand revealing that the complexes are much more stable than ligand. The molar conductance values of the complexes in DMF solvent lay in the range of 12-15 Ω^{-1} cm^2 mol^{-1} (at 25 °C), which indicates that the complexes are non-electrolytes, which agreed with the elemental analysis data and the absence of nitrate and chloride ions. The low conductivity values are in agreement with the low solubility of NXF complexes in water, ethanol, chloroform, acetone and most organic solvents. On the other hand, they are soluble in DMSO and DMF and concentrated acids. The proposed structures of the obtained complexes are shown in Formula II. These structures were confirmed by its analytical data.

3.2 IR spectral analyses

The full tentative assignments of infrared bands of NFX and the obtained complexes are presented in Table 2 and Fig. 1, and have been

compared with those of the free ligand NFX, in order to determine the site of coordination that may be involved in chelation. Table 3 gives the characteristic IR peaks of NFX and its complexes. The infrared spectrum of free NFX exhibits two characteristic bands at 1727 and 1716 cm^{-1} which are assigned to the stretching vibration of the carboxylic group, $\nu(C=O)_{carb}$ [27,28]. These bands are shifts or disappears in the complexes which indicative of the involvement of the carboxyl group in the interaction with metal ion. The spectral region between 1630 and 1350 cm^{-1} is very congested which complicate the assignment of the stretching modes of ligated carboxylato group. The band around 1630 cm^{-1} in the spectra of the two complexes can be assigned to the asymmetric stretching vibration ($\nu C=O_{asym.}$) of the ligated carboxylato group. The two complexes also show another strong or medium strong intensity bands at 1390 and 1430 cm^{-1}, these bands are absent or weak in its intensity in the spectrum of NFX and may be assigned to the symmetric vibration of the ligated COO^{-} group. The $\nu(C=O)$ in the spectrum of NFX appears at 1630 cm^{-1} but in the spectra of the complexes, the $\nu(C=O)$ is effected by the interaction with the metal ion. **Deacon and Phillips 1980 [29],** investigate the asymmetric and symmetric stretching vibration of large number of carboxylato complexes with known crystal structure, and they have studied the criteria that can be used to distinguish between the three binding states of the carboxylate complexes. These criteria are:

(a) Uindentate complexes; $\Delta\nu > 200$ cm^{-1} (where $\Delta\nu$ is the frequency separation between the asymmetric and symmetric stretching of carboxylato group, $[\nu_{asym.}(COO^{-})-\nu_{sym.}(COO^{-})])$. This relation was found in case of monodentate carboxylato complexes.

(b) Bidentate or chelating carboxylato complexes; exhibit $\Delta\nu$ significantly smaller than ionic values ($\Delta\nu < 100$ cm^{-1}).

(c) Bridging complexes; show $\Delta\nu$ comparable to ionic values ($\Delta\nu \sim 150$ cm^{-1}).

Therefore, the difference value $\Delta\nu$ is a useful characteristic for determining the coordination mode of the carboxylate group of the ligands. The observed $\Delta\nu$ for ZrO^{2+} and UO$_2^{2+}$ complexes is around 200 cm^{-1} (Table 3) which suggest a monodentate coordination mode of the carboxylato group. The most important changes during the transformation of NFX into metal complexes take place within the range 650-400 cm^{-1}. The spectra of the synthesized complexes display a group of bands with different intensity which characteristics for

ν(M-O) stretching vibrations of coordinated carboxylato oxygen atom and carbonyl oxygen atom. The ν(Zr-O) and ν(U-O) bands observed at 537 and 536 cm^{-1}, respectively. The spectra of the two complexes show broad water bands around 3500 cm^{-1} confirm the presence of water molecules. The ν_{as}(Zr=O) and ν_{as}(U=O) absorption band occurs as a medium singlet band at 930 cm^{-1}, where the ν_s(Zr=O) and ν_s(U=O) absorption bands occur as a medium-weak singlet band at 830 cm^{-1}. These assignments for the stretching vibrations of the zirconyl (ZrO) and uranyl group (UO$_2$) agree quite well with those known for many oxo-zirconium and dioxo-uranium complexes.

According to the IR spectral data, the NFX is coordinated to the metal ions as a bidentate ligand via one-carboxylato oxygen atoms and the oxygen atom of the pyridine carbonyl group [30]. The most probably structures of the obtained complexes are shown in Formula II. In the [UO$_2$(NFX)$_2$]·9H$_2$O complex, the four oxygen atoms of the two NFX ligands occupy equatorial positions around the central metal atom U(VI), forming a plane containing the four-member ring and the two oxygen atoms of the uranyl group occupy axial positions.
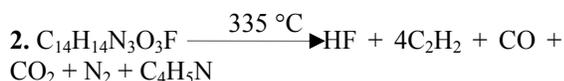
3.3 Thermal analysis

The NFX complexes with ZrO^{2+} and UO$_2^{2+}$ are stable at room temperature and can be stored for several months without any changes. The obtained complexes were studied by thermogravimetric (TG) and differential thermogravimetric (DTG) analysis form ambient temperature to 900 °C N$_2$ atmospheres. The TG curves were redrawn as mg mass loss versus temperature (TG) curves and as the rate of loss of mass versus temperature (DTG) curves. Typical TG and DTG curves are presented in Fig. 2, and the thermoanalytical results are summarized in Table 4. The overall loss of mass from TG curves is 99.94% for NFX, 70.38% for [ZrO(NFX)$_2$].4H$_2$O, 75.54% for [UO$_2$(NFX)$_2$].9H$_2$O. All the complexes show two or three stages of mass loss in their TG/DTG curves, and all mass loss in these stages is due to the decomposition of counter ions and NFX molecules. The found weight loss associated with each step of decomposition for each complex agrees well with the calculated weight loss. The results of TG-DTA agreed with that of elemental analysis. The final products of the complexes obtained at 900°C were confirmed with infrared spectra.

3.3.1 NFX ligand

The data obtained indicate that the NFX is thermally stable in the temperature range 25-50°C. Decomposition of NFX start at 50°C and finished at
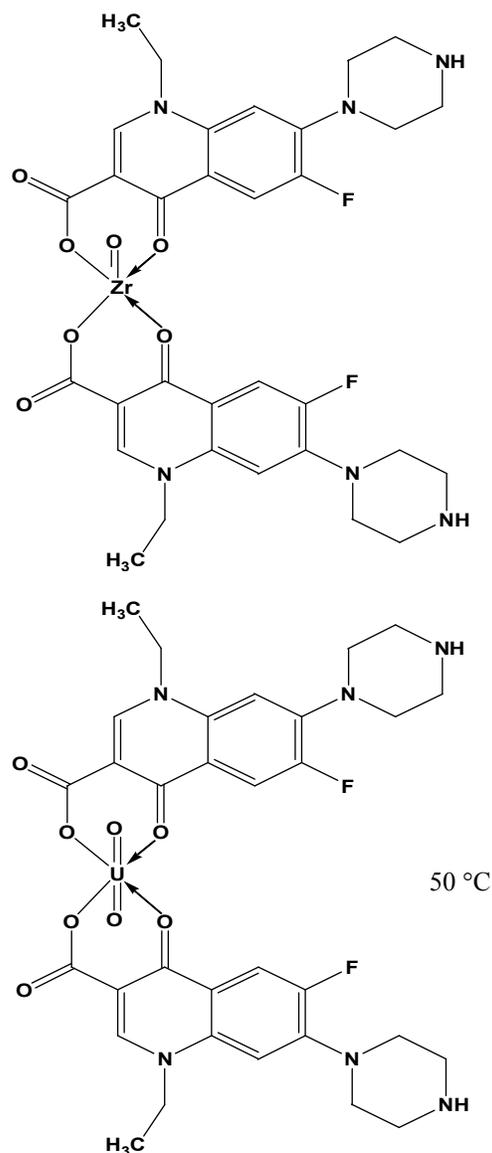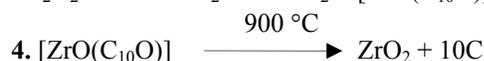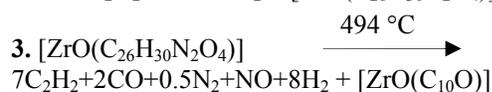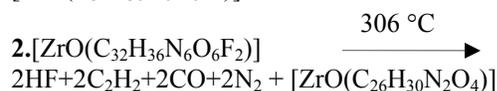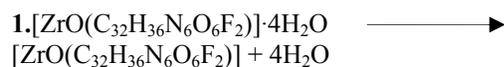
726°C with three stages. The first stage of decomposition occurs between 25 and 270°C, at maximum temperature of 125°C, and is accompanied by weight loss of 8.58%, corresponding exactly to the loss of ethylene molecule (C_2H_4). The second stage of decomposition starts at 270°C and end at 575°C, showing an endothermic peak at 335°C. This stage is accompanied by a weight loss of 69.80%, corresponding to the loss of $4C_2H_2+HF+N_2+CO+CO_2$. The final decomposition step occurs in the range 575-720°C with a maximum at 650°C, and is accompanied by a weight loss of 21.56%, and may be attributed to the loss of pyrrole ring, $2C_2H_2+0.5N_2+0.5H_2$, in reasonable agreement with the theoretical value of 21.0%. The actual weight loss from these three stages is equal to 99.94%, very closer to calculated value 99.80%. The decomposition mechanism proposed for NFX is summarized as follows:

1. $C_{16}H_{18}N_3O_3F \longrightarrow C_2H_2 + C_{14}H_{14}N_3O_3F$

2. $C_{14}H_{14}N_3O_3F \xrightarrow{335\,°C} HF + 4C_2H_2 + CO + CO_2 + N_2 + C_4H_5N$

3. $C_4H_5N \xrightarrow{650\,°C} 2C_2H_2 + 0.5H_2 + 0.5N_2$

3.3.2 [ZrO(NFX)₂]·4H₂O

        The thermal decomposition of [ZrO(NFX)$_2$]·4H$_2$O complex proceeds approximately in three main degradation steps in 25-900°C temperature range, one is dehydration process and the two others is decomposition process. The first dehydration stage of degradation is accompanied by endothermic peak occurs at maximum temperature of 50°C (DTG), in the temperature range 25-180°C. The mass loss in this stage is found to be 9.53%, corresponding to the loss of four water molecules. This is followed by another mass loss (25.21%) in the temperature range 180-400°C, by giving an endothermic effect (DTG$_{max}$, 306°C), corresponding to the loss of $2HF+2C_2H_2+2CO+2N_2$. The third decomposition step occurs at the maximum temperature of 494°C and is accompanied by a weight loss of 35.64%, corresponding to the loss of $7C_2H_2+2CO+ 0.5N_2+NO+8H_2$, then the final thermal product obtained at 900°C is ZrO$_2$ with some carbon atoms. Reported data on thermal analysis studies in the nitrogen atmosphere indicate that ZrO^{2+}/NFX complex decompose to give metal oxide as final product, with few carbon atoms indicates that no sufficiently of oxygen atoms helps to evolved

carbon as carbon monoxide or dioxide. Accordingly, the proposed mechanism for the decomposition of ZrO^{2+}/NFX complex can be summarized as follows:

1. [ZrO($C_{32}H_{36}N_6O_6F_2$)]·4H$_2$O $\longrightarrow$ [ZrO($C_{32}H_{36}N_6O_6F_2$)] + 4H$_2$O

2. [ZrO($C_{32}H_{36}N_6O_6F_2$)] $\xrightarrow{306\,°C}$ 2HF+2C$_2$H$_2$+2CO+2N$_2$ + [ZrO($C_{26}H_{30}N_2O_4$)]

3. [ZrO($C_{26}H_{30}N_2O_4$)] $\xrightarrow{494\,°C}$ 7C$_2$H$_2$+2CO+0.5N$_2$+NO+8H$_2$ + [ZrO($C_{10}O$)]

4. [ZrO($C_{10}O$)] $\xrightarrow{900\,°C}$ ZrO$_2$ + 10C

Formula II. Suggested structure of Zr(IV) and U(VI)-NFX complexes.

3.3.3 [UO$_2$(NFX)$_2$]·9H$_2$O

The thermal analysis curves of [UO$_2$(NFX)$_2$]·9H$_2$O complex show that decomposition takes places in two stages. The first stage is exothermic stage occurs at maximum temperature 45 °C. The weight loss in this stage is 15.49% in the 25-195 °C range corresponding to the loss of 9H$_2$O. The following stage occurs at maximum temperature of 380 °C in the temperature range 195-900°C corresponding to the decomposition of two molecules of NFX. The final thermal product obtained at 900 °C is UO$_2$. Accordingly, the proposed mechanism for the decomposition of UO$_2^{2+}$/NFX complex can be summarized as follows:

1.[UO$_2$(C$_{32}$H$_{36}$N$_6$O$_6$F$_2$)]·9H$_2$O $\longrightarrow$
[UO$_2$(C$_{32}$H$_{36}$N$_6$O$_6$F$_2$)] + 9H$_2$O   45 °C

                                380 °C
2.[UO$_2$(C$_{32}$H$_{36}$N$_6$O$_6$F$_2$)] $\longrightarrow$
2HF+14C$_2$H$_2$+4CO+2N$_2$+2NO+3H$_2$+UO$_2$
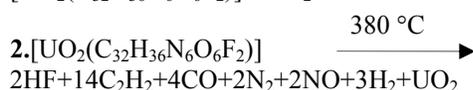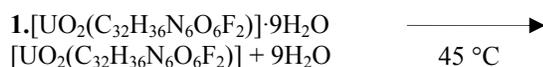
3.4 Kinetic data

In recent years, there has been increasing interest in determining the rate-dependent parameters of solid-state non-isothermal decomposition reactions by analysis TG curves. Several equations **[31-38]** have been proposed as means of analyzing a TG curve and obtaining values for kinetic parameters. The most commonly used methods for this purpose are the differential method of **Freeman and Carroll 1958 [31]**, integral method of **Coats and Redfern 1964 [33],** and the approximation method of **Horowitz and Metzger 1963[36].** In the present study the general thermal behaviors of the NFX ligand and the two complexes in terms of stability ranges, peak temperatures and values of kinetic parameters, are shown in Fig. 3, and Table 5. The kinetic parameters have been evaluated using the following methods and the results obtained by these methods are compared with one another. The following two methods are discussed in brief.

3.4.1 Coats-Redfern (CR) method

The Coats-Redfern equation (1), which is atypical integral method, can be represented as:

$$\int_0^\alpha d\alpha/(1-\alpha)^n = (A/\varphi)\int_{T_1}^{T_2} e^{-E^*/RT}\,dT \qquad (1)$$

For convenience of integration, the lower limit T_1 is usually taken as zero. This equation on integration gives:

$$Ln[-\ln(1-\alpha)/T^2] = -E^*/RT + \ln[AR/\varphi E] \qquad (2)$$

where α is the fraction of the sample decomposed at time T, T is the derivative peak temperature, A is frequency factor, R is the gas constant, E^* is the activation energy and φ is the linear heating rate. A

plot of left-hand side (LHS) against $1/T$ was drawn. E^* is the energy of activation in KJ mol^{-1} and calculated from the slop and A in (s^{-1}) from the intercept. The entropy of activation ΔS^* in (JK^{-1} mol^{-1}) was calculated by using the following equation:

$$\Delta S^* = R\ln(Ah/kT_s) \qquad (3)$$

where k is the Boltzmann constant, h is the Plank's constant and T_s is the DTG peak temperature.

3.4.2 Horowitz-Metzger (HM) approximation method

The Horowitz-Metzger equation (4) was written in the form as follows:

$$Log[\log(w_\alpha/w_\gamma)] = E^*\theta/2.303RT_s^2 - \log 2.303 \qquad (4)$$

where $\theta = T - T_s$, $w_\gamma = w_\alpha - w$, w_α = mass loss at the completion of the reaction; w = mass loss up to time t. The plot of Log[log (w_α/w_γ)] versus θ was drawn and found to be linear from the slope E^* was calculated. The pre-exponential factor, A, was calculated from the Eg. (5):

$$E^*\theta/RT_s^2 = A/[\varphi \exp(-E^*/RT_s)] \qquad (5)$$

From the TG curves, the activation energy, E^*, entropy of activations, ΔS^*, enthalpy activations, ΔH^*, and Gibbs free energy, ΔG^*, were calculate from;

$\Delta H^* = E^* - RT$
$\Delta G^* = \Delta H^* - T\Delta S^*$

From Table 5, the following outcomes are draw:

1 The results show that the kinetic data obtained by the two methods are comparable and in harmony with each other.

2 Higher value of activation energy suggests the higher thermal stability. The ZrO^{2+}/NFX show higher value of activation energy than UO$_2^{2+}$/NFX, indicating higher thermal stability of this complex.

3 The activation energy of ZrO^{2+} and UO$_2^{2+}$ complexes is expected increase with decreasing metal ion radium **[39-42]**. The calculated ΔE^* values using Coats-Redfern method for the first decomposition stage of the complexes are found to be E^* Zr(IV)= 1.57x10^4 kJmol^{-1} > E^* U(VI)= 1.36x10^4 kJmol^{-1}, which is in accordance with r U(VI)= 156 pm < r Zr(IV)= 160 pm,

4 The ΔS^* values of the main stage for the two complexes were found to be negative which indicates that the reaction rates are slower than normal **[43]**. Furthermore, these data indicate that the activated complexes have more ordered structure than the reactants.

5 The satisfactory values of correlation coefficients of the Arrhenius plots (r) of the thermal decomposition steps were found to be (r ~ 0.9) in all cases indicate good fit with linear function and reasonable agreement between

experimental data and the values of kinetic parameters.

6 It is clear that the thermal decomposition process of the two complexes is non-spontaneous, i.e., the complexes are thermally stable.

Table 1. Elemental analysis and physical properties of the NFX and its complexes.

Compound	Molecular weight	Yield (%)	Color	mp (°C)	Analysis (%) found (calculated)				Λ ($\Omega^{-1}cm^2mol^{-1}$)
					C	H	N	M	
NFX	319	-	Yellow	232	59.45 (60.18)	5.54 (5.68)	12.89 (13.16)	-	10.16
[ZrO(NFX)$_2$]·4H$_2$O	817	76	White	> 300	47.23 (47.00)	5.28 (5.39)	10.50 (10.28)	11.46 (11.14)	12.5
[UO$_2$(NFX)$_2$]·9H$_2$O	1070	77	Yellow	> 300	35.34(35.89)	5.21(5.05)	8.03 (7.85)	29.87 (30.65)	15.0

Table 2. Infrared frequencies[a] (cm^{-1}) and tentative assignments[b] for NFX and its complexes.

NFX ligand	ZrO^{2+} complex	UO$_2^{2+}$ complex	Assignments
3399 ms	3747 ms, 3712 vw, 3674 m, 3649 m 3613 vw, 3588 vw, 3502 br, ms	3712 w, 3674 w, 3650 w, 3503 br	ν(N-H) + ν_{as}(O-H); H$_2$O
3267 vw, 3228 vw, 3189 vw, 3130 vw 3021 w, 2927 m, 2823 w, 2796 w 2764 w, 2723 m, 2696 w, 2654 w 2617 w, 2511 w, 2468 m	3040 br, ms, 2850 mw, 2736 mw 2516 mw, 2364 ms, 2338 sh, ms	3023 br, 3023 br, 2925 w, 2850 w 2486 w, 2366 m, 2340 sh, m	ν(C-H), ν(N-H), ν(-$\overset{+}{N}H_2$)
1727 sh, 1716 ms	1794 vw, 1719 vs	1720 vs	ν(C=O): (OCO$^-$)
1630 vs, 1620 sh	1629 vs	1630 vs	ν(C=O) + δ_b(H$_2$O)
1595 w, 1552 w	1541 w	1541 m	Phenyl breathing modes
1482 vs, 1454 m	1497 vw	1495 vs,	CH; deformation of -CH$_2$-
1396 s	1460 vs , 1393 m	1459 vs , 1390 m, 1340 m	ν_s(COO$^-$) + ν(N-O): NO$_3^-$
1307 vw	1339 m, 1303 mw	1304 mw	δ_b(CH$_2$)
1277 vw, 1263 s	1271 s	1271 s	ν(C-C)
1248 vw, 1201 m	1215 mw	1213 w	ν(C-O)
1192 m	1178 mw	1178 m	ν(C-N)
1153 vw, 1142 w 1132 w, 1115 w, 1095 m, 1076 m 1051 vw, 1036 ms, 1024 w, 1005 m 982 m	1144 mw, 1105 mw, 1077 vw, 1029 m	1143 m, 1104 w, 1076 w, 1030 ms	δ_r(CH$_2$)
972 w, 935 ms, 916 m, 899 m 887 m, 858 w, 823 ms, 804 ms	939 m, 892 ms, 831 mw, 805 mw	939 ms, 896 s, 832 mw, 805 m	CH- bend; phenyl
750 s, 706 m	775 mw, 746 m, 705 w	776 mw, 747 m, 706 w	δ_b(COO$^-$)
667 w, 631 w, br 569 ms, 524 w, 499 m, 474 m 453 vw, 430 ms	668 w, 621 w, 537 mw 470 mw, 417 mw	667 w, 621 w, 536 m 409 w, 415 w	ν(M-O) ring; δ_r rocking deformation

[a] s, strong; w, weak; m, medium; sh, shoulder; v, very; br, broad.
[b] ν, stretching; δ_b, bending; δ_r, rocking.

Table 3. Characteristic IR peaks (cm^{-1}) of NFX and its complexes

| Compound	ν(N-H)	ν(C=O)$_p$	ν(COO$^-$) (asym.)	ν(COO$^-$) (sym.)	$\Delta\nu$ (asym.-sym.)	(M-O)
NFX	3399	1727	1620	-	-	-
NFX/ZrO^{2+}	3502	1719	1629	1430	199	537
NFX/UO$_2^{2+}$	3503	1720	1630	1429	201	536

Table 4. Thermo analytical data for NFX and its complexes

Compound	Decomposition	TG results temp. range (°C)	T$_{max}$ (°C)	Weight loss (%)		Lost species
				Found	Calculated	
NFX C$_{16}$H$_{18}$N$_3$O$_3$F	First step	25-270	125	8.58	8.78	C$_2$H$_4$
	Second step	270-575	335	69.80	70.22	HF+4C$_2$H$_2$+CO+CO$_2$+N$_2$
	Third step	575-726	650	21.56	20.80	2C$_2$H$_2$+0.5H$_2$+0.5 N$_2$
	Total loss, Residue	-	-	99.94, 0.0	99.80, 0.0	-
[ZrO(NFX)$_2$]·4H$_2$O	First step	25-180	50	9.53	8.81	4H$_2$O
	Second step	180-400	306	25.21	24.97	2HF+2C$_2$H$_2$+2CO+2N$_2$
	Third step	400-900	494	35.64	36.47	7C$_2$H$_2$+2CO+0.5N$_2$+NO+8H$_2$
	Total loss, Residue	-	-	70.38, 29.62	70.25, 29.74	ZrO$_2$, 10C
[UO$_2$(NFX)$_2$]·9H$_2$O	First step	25-195	45	15.49	15.14	9H$_2$O
	Second step	195-900	380	60.05	59.63	2HF+14C$_2$H$_2$+4CO+2N$_2$+2NO+ 3H$_2$
	Total loss, Residue	-	-	75.54, 24.46	74.77, 25.23	UO$_2$

Table 5. Thermo analytical data for NFX and its complexes determined using Coats-Redfern (CR) and Horowitz-Metzger (HM).

Compound	Stage	Method	Parameters [a]					r
			E^*	A	ΔS^*	ΔH^*	ΔG^*	
NFX	1st	CR	9.36×10^4	2.00×10^1	-5.01×10^1	9.03×10^4	1.10×10^5	0.98530
		HM	9.66×10^4	8.68×10^1	-3.79×10^1	9.33×10^4	1.08×10^5	0.98170
ZrO^{2+}/NFX	1st	CR	1.57×10^4	0.678	-2.15×10^2	1.25×10^4	1.08×10^5	0.89296
		HM	2.23×10^4	5.380	-2.33×10^2	1.91×10^4	1.07×10^5	0.90901
UO$_2$$^{2+}$/NFX	1st	CR	1.36×10^4	0.296	-2.57×10^2	1.06×10^4	1.02×10^5	0.88324
		HM	1.72×10^4	1.340	-2.44×10^2	1.42×10^4	1.01×10^5	0.90922

[a] Units of parameters: E in kJ mol^{-1}, A in s^{-1}, ΔS in J mol^{-1}K^{-1}, ΔH and ΔG in kJ mol^{-1}.
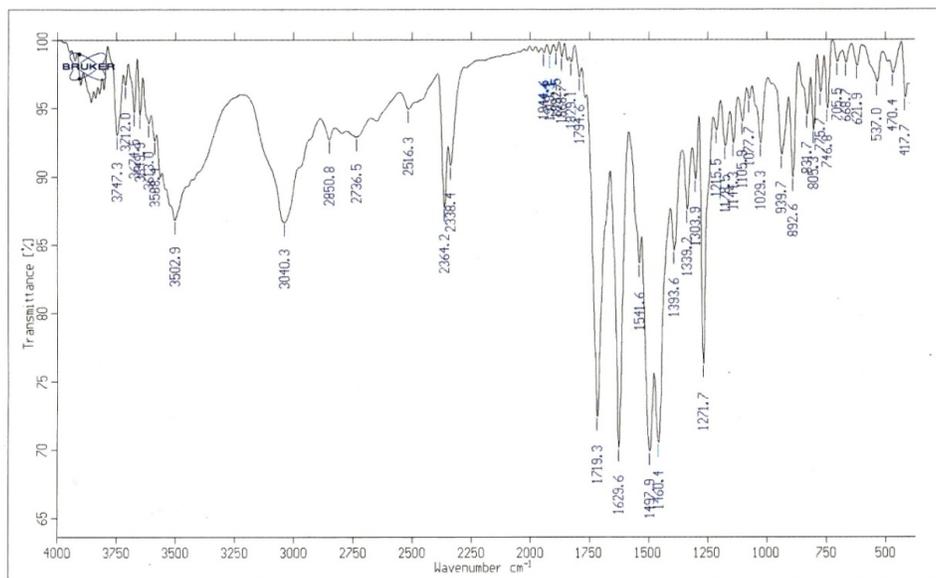
Fig. 1 (A) Infrared spectra of [ZrO(NFX)$_2$]·4H$_2$O complex.
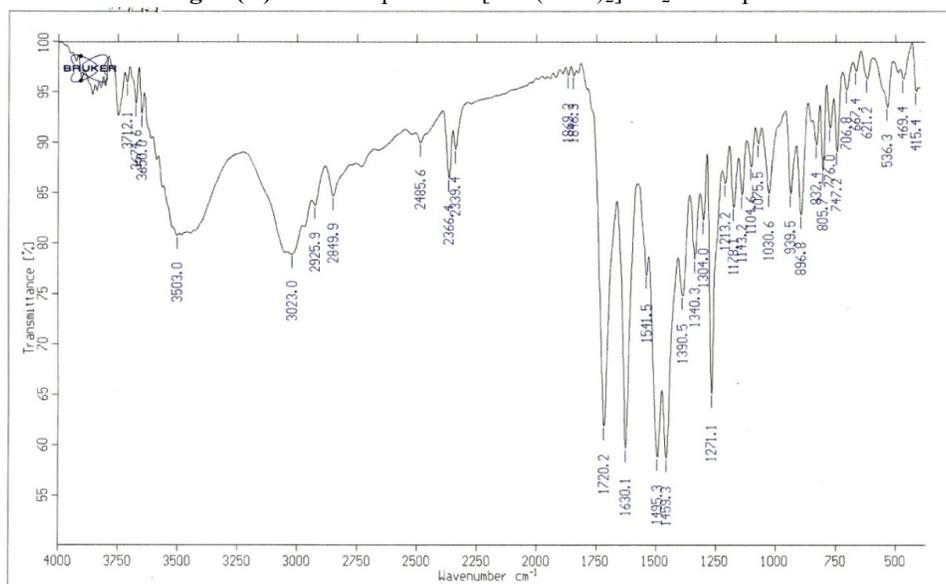
Fig. 1 (B) Infrared spectra of [UO$_2$(NFX)$_2$]·9H$_2$O complex.
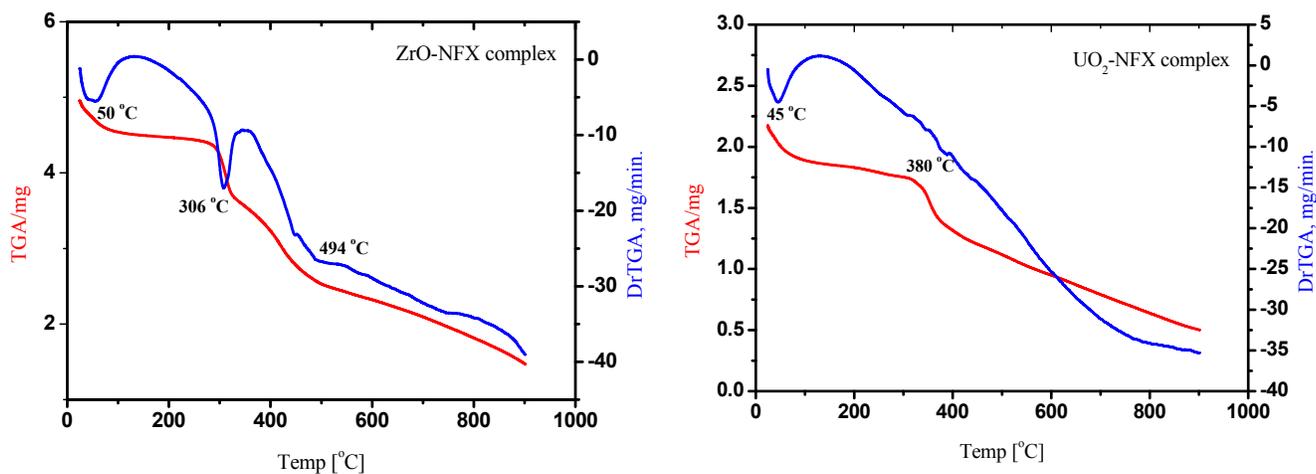
Fig. 2 TG and DTG curves of NFX complexes.
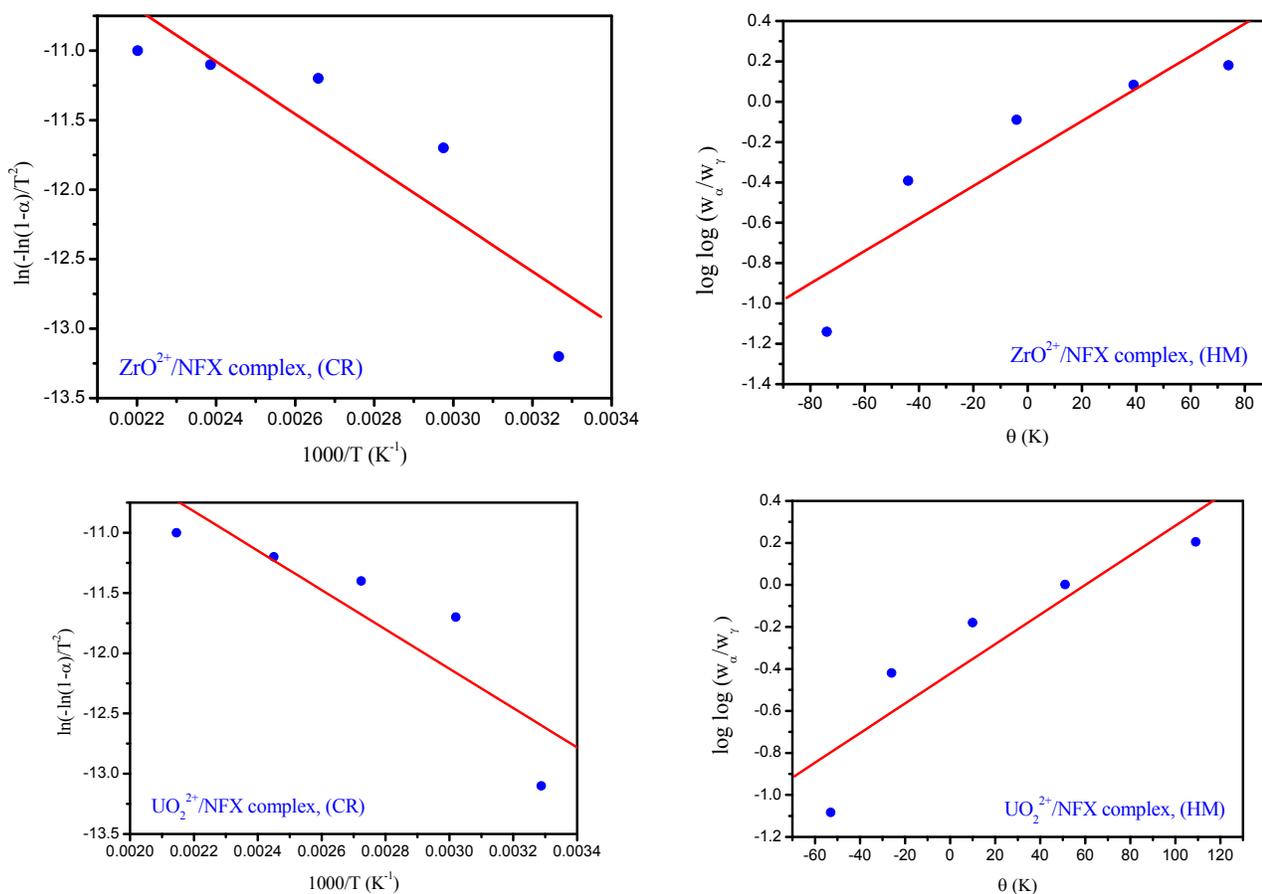
Fig. 3 The diagrams of kinetic parameters of NFX complexes using Coats-Redfern (CR) and Horowitz-Metzger (HM) equations.

Corresponding Author:
El-Megharbel S. M.
Department of Chemistry, Faculty of Science, Zagazig University, Zagazig, Egypt
samyelmegharbel@yahoo.com.

References
[1] Dhaneshwar,S., K.,S. Tewari, D. Joshi, P. Godbole, K.Ghosh,(**2011**) Chemistry and Physics of Lipids 164 307-313.
[2] Van BambekeF., J.M., J.Michot, P.M. Van Eldere, A.Tulkens,(**2005**) Clinical Microbiology and Infection 11 (**256-280**.
[3]. GoyalR.N., A.R.S. Rana, H. Chasta,(**2012**) Bioelectrochemistry 83 (**46-51**).
[4] Rahman,N., Y. Ahmed, S.N.H. Azmi, (**2004**) European Journal of Pharmaceutics and Biopharmacetics (359-367).
[5] Ballesteros,O., I. Toro, V. Sanz-Nebot, A. Navalon, J.L. Vilchez, J. Barbosa, (**2003**) Journal of Chromatography B 798 (137-144).
[6] Yang,W., Y. Lu, F. Zheng, X. Xue, Na Li, D. Liu, (**2012**) Chemical Engineering Journal 179 (112-118).
[7] LiuW., J. Zhang, C. Zhang, L. Ren, (**2011**) Chemical Engineering Journal 171 (431-438).
[8]. MoreV.R., U.S. Mote, S.R. Patil, G.B. Kolekar, (**2009**) Spectrochimica Acta Part A 74 (771-775).
[9] Ni Y.N., Y. Wang, S. Kokot, (**2008**) Spectrochimica Acta Part A 70 (1049-1059).
[10] TongC.L., G.H. Xiang, Journal of Fluorescence 16 (**2006**) 831-837.
[11] HuangK.J., X. Liu, W.Z. Xie, H.X. Yuan, (**2008**) Colloids and Surfaces B: Biointerfaces 64 (269-274).
[12CuiJ., K. Zhang, Q. Huang, Y. Yu, X. Peng, (**2011**) Analytical Chimica Acta 688 (84-89).
[13] Refat,M.S., W.F. El-Hawary, M.A. Mohamed, (**2012**) Journal of Molecular Structure 1013 (45-54).
[14]. Shaikh,R., R. Giridhar, M.R. Yadav, (**2007**) International Journal of Pharmaceutics 332 (24-30).
[15] Efthimiadou,N., G. Psomas, Y. Sanakis, N. Katsaros, A. Karaliota, (**2007**) Journal of Inorganic Biochemistry 101 (525-535).
[16]. Refat,M.S., (**2007**) Spectrochimica Acta Part A 68 (1393-1405).
[17] Adam,A., (**2012**) Journal of Materials Science Research 1 (167-182).
[18] Sadeek,A., W.H. El-Shwiniy, W.A. Zordok, A.M. El-Didamony, (**2009**)The Journal of the Argentine Chemical Society 97, 2 (128-148).
[19] Sadeek, A.,A.M El-Didamony, W.H. El-Shwiniy, W.A. Zordok, (**2009**) The Journal of the Argentine Chemical Society 97, 2 (51-76).
[20] Sadeek,A., (**2005**) Journal of Molecular Structure 753 (1-12).
[21] Sunduru,N., L. Gupta, K. Chauhan, N.N. Mishra, P.K. Shukla, P.M.S. Chauhan, (**2011**) European Journal of Medicinal Chemistry 46 (1232-1244).
[22] Dhaneshwar,S., K. Tewari, S. Joshi, D. Godbole, P. Ghosh, (**2011**) Chemistry and Physics of Lipids 164 (307-313).
[23] Patel, M.N., H.N. Joshi, C.R. Patel, (**2012**) Journal of Organometallic Chemistry 701 (8-16).
[24] Ture,L.I., L. Golic, P. Bukovec, M. Gubina, (**1998**)Journal of Inorganic Biochemistry 71 (53-60).
[25] Pei,Z., J. Kong, X. Shan, B. Wen, (**2012**) Journal of Hazardous Materials 203-204 (137-144).
[26]Haque,M.M., M. Muneer, (**2007**)Journal of Hazardous Materials 145 (51-57).
[27] Ture,L.I., I. Leban, G. Klintschar, N. Bukovec, S. Zalar, (**1997**) Journal of Inorganic Biochemistry 66 (77-82).
[28] Ture,L.I., I. Leban, N. Bukovec, (**1997**) Journal of Inorganic Biochemistry 66 (241-245).
[29] Deacon,G.B., R.J. Phillips, (**1980**) Coordination Chemistry Reviews 33 (227-250).
[30] Ture,L.I., (**2002**) Coordination Chemistry Reviews 232 (27-47).
[31] Freeman,E.S., B. Carroll, (**1958**) Journal of Physical Chemistry 62 (394-397).
[32]. Sestak,J., V. Satava, W. Wendlandt, (**1973**) Thermochimica Acta 7 333.
[33] Coats,A. W., P.Redfern (**1964**) Nature (68).
[34] Ozawa, T., (**1965**) Bulletin of the Chemical Society of Japan 38 (1881-1886).
[35] Wendlandt, W.W.,(**1974**) Thermal Methods of Analysis, Wiley, New York.
[36] Horowitz, H.W.,G. Metzger, (**1963**)Anal. Chem. 35 (1464-1468).
[37] Flynn, J.H., A. Wall, (**1966**) Polymer Letters 4(323).
[38] Kofstad, P., (**1957**) Nature 179 (1362).
[39] Avsar, G., N. Kulcu, H. Arslan, (**2002**) Turkish Journal of Chemistry 26 (607-616).
[40] Tunali, N.K., S. Ozkar,(**1963**) Inorg. Chem., Hazi University Publication, Ankara, Turkey, Pub. No. 185.
[41] Arslan, H., U. Florke, N. Kulcu, M.F. Emen, (**2006**) Journal of Coordination Chemistry 59 (2) 223.
[42] Frost, A.A., R.G. Pearson, (**1961**) Kinetics and Mechanism, Wiley, New York, NY, USA.
[43] Quan, C.X., L.H. Bin, G.G. Bang, (**2005**) Materials Chemistry and Physics 91 (317-324).

7/7/2012